REPORT DOCUMENTATION PAGE

Form Approved OMB NO. 0704-0188

1. REPORT DATE (DD-MM-YYYY)	2. REPORT TYPE	3. DATES COVERED (From - To)
27-02-2017	Final Report	1-Jul-2011 - 30-Sep-2016

4. TITLE AND SUBTITLE
Final Report: Composite Films of Metal Oxide and Carbon Nanostructures for Energy Storage

5a. CONTRACT NUMBER

5b. GRANT NUMBER
W911NF-04-D-0001

5c. PROGRAM ELEMENT NUMBER
611102

6. AUTHORS
Gyeonghee Lee, Chakrapani V. Varanasi, and Jie Liu,

5d. PROJECT NUMBER

5e. TASK NUMBER

5f. WORK UNIT NUMBER

7. PERFORMING ORGANIZATION NAMES AND ADDRESSES
Duke University
C/O Office of Research Support
2200 W. Main St., Ste. 710
Durham, NC 27705 -4677

8. PERFORMING ORGANIZATION REPORT NUMBER

9. SPONSORING/MONITORING AGENCY NAME(S) AND ADDRESS (ES)
U.S. Army Research Office
P.O. Box 12211
Research Triangle Park, NC 27709-2211

10. SPONSOR/MONITOR'S ACRONYM(S)
ARO

11. SPONSOR/MONITOR'S REPORT NUMBER(S)
59752-MS-SR.14

12. DISTRIBUTION AVAILIBILITY STATEMENT
Approved for Public Release; Distribution Unlimited

13. SUPPLEMENTARY NOTES
The views, opinions and/or findings contained in this report are those of the author(s) and should not contrued as an official Department of the Army position, policy or decision, unless so designated by other documentation.

14. ABSTRACT
Rechargeable batteries and supercapacitors are two major systems for electrochemical energy storage. Some battery technologies are mature, while supercapacitors and other advanced battery technologies are currently at earlier stages of development, simply due to far lower energy densities compared to current established systems. In spite of their different abilities in energy and power performances, especially, rechargeable batteries and pseudocapacitors have similarities in configuration and charge storage mechanisms, which involve reversible redox reactions in transition metal based electrode materials. Thus, their charge storage capacity as well as rate capability largely

15. SUBJECT TERMS
supercapacitors,electrocatalysts, energy storage, oxide/carbon nanotube composites

16. SECURITY CLASSIFICATION OF:			17. LIMITATION OF ABSTRACT	15. NUMBER OF PAGES	19a. NAME OF RESPONSIBLE PERSON
a. REPORT	b. ABSTRACT	c. THIS PAGE			Chakrapani Varanasi
UU	UU	UU	UU		19b. TELEPHONE NUMBER 919-549-4325

Standard Form 298 (Rev 8/98)
Prescribed by ANSI Std. Z39.18

Report Title

Final Report: Composite Films of Metal Oxide and Carbon Nanostructures for Energy Storage

ABSTRACT

Rechargeable batteries and supercapacitors are two major systems for electrochemical energy storage. Some battery technologies are mature, while supercapacitors and other advanced battery technologies are currently at earlier stages of development, simply due to far lower energy densities compared to current established systems. In spite of their different abilities in energy and power performances, especially, rechargeable batteries and pseudocapacitors have similarities in configuration and charge storage mechanisms, which involve reversible redox reactions in transition metal based-electrode materials. Thus, their charge storage capacity as well as rate capability largely depend on ion and electron transport kinetics within electrode materials. These transport kinetics, however, are often limited since the most of the transition metal-based materials have intrinsically poor electrical conductivity. In this work, to understand the influence on the electrode conductivity and electrochemical performances in these systems, a systematic study was conducted using three main approaches namely nanostructuring, chemical substitutions, and introduction of carbon additives.

Enter List of papers submitted or published that acknowledge ARO support from the start of the project to the date of this printing. List the papers, including journal references, in the following categories:

(a) Papers published in peer-reviewed journals (N/A for none)

Received		Paper
02/27/2017	4	Yingwen Cheng,Hongbo Zhang, Chakrapani V. Varanasiac and Jie Liu. Improving the Performance of Cobalt-Nickel Hydroxides-based Self-Supporting Electrodes for Supercapacitors using Accumulative Approaches, Energy & Environmental Science, (06 2013): 3314. doi:
02/27/2017	12	Gyeonghee Lee, Xiao Zhang, Hongbo Zhang, Chakrapani V. Varanasi, Jie Liu. Effect of interlayer spacing on sodium ion insertion in nanostructured titanium hydrogeno phosphates/carbon nanotube composites, RSC Adv., ( ): 60015. doi:
TOTAL:	**2**	

Number of Papers published in peer-reviewed journals:

(b) Papers published in non-peer-reviewed journals (N/A for none)

Received		Paper
TOTAL:		

Number of Papers published in non peer-reviewed journals:

(c) Presentations

Number of Presentations: 0.00

Non Peer-Reviewed Conference Proceeding publications (other than abstracts):

Received Paper

TOTAL:

Number of Non Peer-Reviewed Conference Proceeding publications (other than abstracts):

Peer-Reviewed Conference Proceeding publications (other than abstracts):

Received Paper

TOTAL:

Number of Peer-Reviewed Conference Proceeding publications (other than abstracts):

(d) Manuscripts

Received Paper

TOTAL:

Number of Manuscripts:

Books

Received Book

TOTAL:

Received	Book Chapter

TOTAL:

Patents Submitted

Patents Awarded

Awards

Graduate Students

NAME	PERCENT_SUPPORTED	Discipline
Gyeonghee Lee	1.00	
FTE Equivalent:	**1.00**	
Total Number:	**1**	

Names of Post Doctorates

NAME	PERCENT_SUPPORTED
FTE Equivalent:	
Total Number:	

Names of Faculty Supported

NAME	PERCENT_SUPPORTED	National Academy Member
Jie Liu	0.00	
FTE Equivalent:	**0.00**	
Total Number:	**1**	

Names of Under Graduate students supported

NAME	PERCENT_SUPPORTED
FTE Equivalent:	
Total Number:	

Student Metrics

This section only applies to graduating undergraduates supported by this agreement in this reporting period

The number of undergraduates funded by this agreement who graduated during this period: 0.00

The number of undergraduates funded by this agreement who graduated during this period with a degree in science, mathematics, engineering, or technology fields:..... 0.00

The number of undergraduates funded by your agreement who graduated during this period and will continue to pursue a graduate or Ph.D. degree in science, mathematics, engineering, or technology fields:..... 0.00

Number of graduating undergraduates who achieved a 3.5 GPA to 4.0 (4.0 max scale):..... 0.00

Number of graduating undergraduates funded by a DoD funded Center of Excellence grant for Education, Research and Engineering:..... 0.00

The number of undergraduates funded by your agreement who graduated during this period and intend to work for the Department of Defense 0.00

The number of undergraduates funded by your agreement who graduated during this period and will receive scholarships or fellowships for further studies in science, mathematics, engineering or technology fields: 0.00

Names of Personnel receiving masters degrees

NAME
Total Number:

Names of personnel receiving PHDs

NAME
Gyeonghee Lee
Total Number: 1

Names of other research staff

NAME	PERCENT_SUPPORTED
FTE Equivalent:	
Total Number:	

Sub Contractors (DD882)

Inventions (DD882)

Scientific Progress

Please see attachment

Technology Transfer

none

Background

The demand for electrical energy is increasing with technological advances in electronics, electric vehicles, and energy production. The majority of today's electrical energy is derived from fossil fuels such as coal, natural gas, and oil.[1] The resources of fossil fuels, however, are depleting and their consumption has brought serious environmental crises such as climate change.[2] Emissions of a greenhouse gas, carbon dioxide (CO_2) are unavoidable in electrical energy production by burning fossil fuels. It is predicted that CO_2 emissions will more than double by 2050.[3] Thus, depending on fossil energy will raise concerns over the energy security. As such, current energy supply is unsustainable not only environmentally but also economically. Moreover, emphasis on low-carbon energy systems has drawn attention to development of energy storage technologies to realize effective use of renewable energy resources and to improve energy use efficiency. Since renewable resources such as solar, wind, and geothermal are intermittent, advanced energy storage technologies are required to bridge the temporal gap between energy supply and demand.[4] Thus, energy storage technologies are valuable components in these purposes.

Energy storage systems

Currently, electrochemical energy storage systems are the most optimal solutions to power various technologies, ranging from compact portable electronics to grid-scale energy storage applications. Among available electrochemical energy storage systems, lithium batteries and supercapacitors are the most promising technologies. They store the electrical energy in the form of chemical energy and deliver it when needed, by reversing the electrochemical reaction. The terms power density and energy density are used to evaluate and compare the rate capability and

the energy content of electrochemical energy storage systems, usually in a graph called Ragone plot.[5] Here, power density represents how fast energy can be delivered and energy density represents how much energy can be stored. A simple Ragone plot indicates that supercapacitors are a high-power system, whereas batteries are a high-energy system.

Supercapacitors

Supercapacitors are power devices that can be fully charge or discharge in seconds. While their energy density (~5 Wh kg^{-1}) is lower than those in batteries, power density (10 kW kg^{-1}) is much higher. They currently, thus, fill the gap between batteries and conventional capacitors. They have had an important role in complementing or replacing batteries in the energy storage field, such as back-up supplies used to protect against power disruption and load-leveling. The electrode materials used as well as the charge storage mechanism are important factors classifying supercapacitors into two types; electrical double layer capacitors (EDLCs) and pseudocapacitors. EDLCs store the charge electrostatically through reversible adsorption of ions of the electrolyte onto electrode materials that are electrochemically stable and have high accessible specific surface area (1000 – 2000 m^2 g^{-1}).[6] This electrostatic charge storage mechanism allows fast energy capture and deliver in a few seconds, and over millions of charge-discharge cycles. Their capacitance, however, is typically ~150 F g^{-1}, which strongly depends on the specific surface area of electrode materials.[7] Pseudocapacitance was discovered by Conway *et al.* in 1975. The charge storage mechanism of pseudocapacitors involves the formation of electrical double layer and fast, reversible redox reactions at the surface of electrode materials.[8] Such surface redox reactions render charge-discharge rates, comparative to those in EDLCs, but much higher specific capacitance. Due to multiple oxidation states presented during redox

reactions, to date, transition metal-based compounds, such as RuO_2, Co_3O_4, MnO_2, V_2O_5, and NiO, have been extensively studied as pseudocapacitive materials.[9-13]

Sodium ion batteries

Lithium-ion batteries (LIBs) have dominated the current battery market. Particularly, their use for electric vehicles has been addressed to replace the gasoline-powered vehicles in order to reduce CO_2 emissions. The market for automotive LIBs is rapidly expanding with the worldwide demand for electric vehicles.[14] The widespread use of such large format LIBs for electric vehicles, combined with concerns on Li abundance, would drive up prices of Li containing chemicals.[15] Li supplies will run out in the future if LIBs are also adopted for grid-scale energy storage applications.[15] As an alternative to LIBs, sodium-ion batteries (NIBs) have the potential to meet the needs in the grid-scale energy storage. Sodium (Na) is the 4th most abundant elements on Earth and shares some chemical properties with Li.[16] Structure, components, system, and charge storage mechanism of NIBs are basically the same as those of LIBs, except for Na ions as charge carriers instead of Li ions.[16] However, not all of the electrode materials that show Li storage can be directly used for Na storage due to the steric limitation caused by the bulkier Na^+ (1.02 Å) compared to Li^+ (0.76 Å).[17] Since NIBs are an emerging technology, the discovery of new materials which enables Na electrochemistry has been still lacking. As battery performances such as specific capacity and operation voltage are mainly determined by the electrochemical properties of electrode materials, the greatest attention should be paid to identify high-performance electrode materials.

Energy storage materials challenges

As discussed earlier, rechargeable batteries and supercapacitors are two major systems for electrochemical energy storage. Some battery technologies are mature, while supercapacitors and other advanced battery technologies are currently at earlier stages of development, simply due to far lower energy densities compared to current established systems (e.g. pumped storage hydropower). Thus, energy densities of both rechargeable batteries and supercapacitors should be further improved to be realized as highly efficient and reliable energy storage systems. In spite of their different abilities in energy and power performances, especially, rechargeable batteries and pseudocapacitors have similarities in configuration and charge storage mechanisms, which involve reversible redox reactions in transition metal based-electrode materials. Thus, their charge storage capacity as well as rate capability largely depend on ion and electron transport kinetics within electrode materials. These transport kinetics, however, are often limited since the most of the transition metal-based materials have intrinsically poor electrical conductivity. Next three sections will discuss three main approaches to improve electrode conductivity and thus, enhance overall electrochemical performances of these systems; nanostructuring, chemical substitution, and introducing carbon additives.

Effects of Morphology and Chemical Doing on Electrochemical Properties of Metal Hydroxides in Pseudocapacitors[1]

Nickel hydroxides ($Ni(OH)_2$), are widely used as electroactive materials in batteries and pseudocapacitors due to their high theoretical capacitance of 2082 F g^{-1} and well-defined redox processes.[18] Hydrotalcite-like $Ni(OH)_2$, particularly, has a larger interlayer distance (~7 Å) than

[1] This work has been published in *Nanoscale* **2015**, 7, 3181 – 3188.

its brucite-like counterpart (~4.6 Å), showing interesting electrochemical activities.[19] Their limited electrical conductivity (10^{-5}–10^{-9} S cm^{-1}), however, has been addressed as the most significant problem obstructing the ideal performance of $Ni(OH)_2$-based electrodes.[20] Thus, developing effective strategies to assemble $Ni(OH)_2$-based electrodes with improved electrical conductivity is desired. In recent years, an extensive research has been carried out to improve the electrode conductivity through chemical doping and morphology control of active materials on the nanoscale. Specifically, the electrode conductivity can be improved by chemical doping through which nickel (Ni) is partially substituted with other cations such as Co, Al, and Zn.[21-23] Substituting Ni with Co particularly improves the electrochemical performance of $Ni(OH)_2$ by increasing the electrical conductivity. For example, the Co doped-$Ni(OH)_2$ electrode exhibited a high specific capacitance up to 1560 F g^{-1}, when the composition of the hydroxide is $Co_{0.5}Ni_{0.5}(OH)_2$.[24] This specific capacitance increase was attributed to the improved electrical conductivity as well as the favorable charge hopping.[24,25] On the other hand, reducing the size of active materials into the nanoscale also enables reduction in resistance due to the decreased transport distance for both electronic and ionic species.[26] It is thus clear that both morphology control and chemical substitution positively affect the electrochemical performance of $Ni(OH)_2$ when applied individually. However, it is unclear whether better electrochemical performances can be achieved when those two approaches are combined. Thus, our study is aimed at elucidating the mechanism and the combined effects of chemical substitution and morphology control on the electrochemical properties of $Ni(OH)_2$ materials.

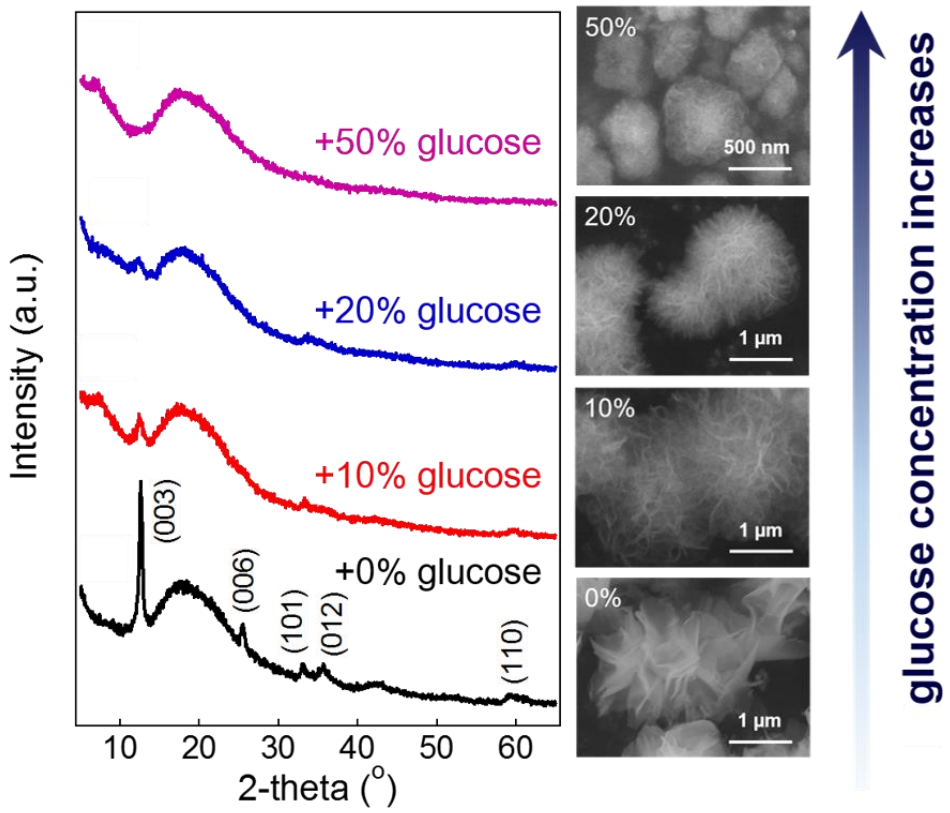

Figure 1: XRD patterns of $Ni(OH)_2$ synthesized with (a) 0%, (b) 10%, (c) 20%, and (d) 50% glucose.

We have shown that the structural features compete with chemical doping in influencing the electrochemical performance of metal hydroxide electrodes. The morphology and the degree of crystallinity of $Ni(OH)_2$ were changed by adding glucose in the ethanol-mediated solvothermal synthesis (**Figure 1**). $Ni(OH)_2$ produced in this manner exhibited an increased specific capacitance due to the reduced particle/flake size as a function of glucose concentration (**Figure 2**). In addition, $Ni(OH)_2$ prepared with glucose showed high water contents both on the surface and in the interlayer galleries. During the alcohol-based solvothermal treatment, glucose undergoes ethanolysis through which α-hydroxyl groups are substituted by ethoxy groups. They, especially at high glucose concentrations, limit the diffusion of Ni precursors during synthesis and therefore inhibit the growth of $Ni(OH)_2$ particles into larger crystals (**Figure 3**).

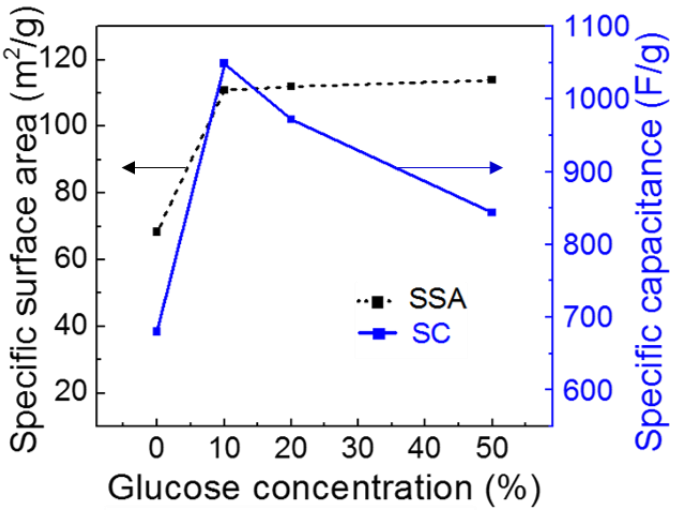

Figure 2: Comparisons of changes in the specific surface area (SSA) and the specific capacitance (SC) of $Ni(OH)_2$ as a function of glucose concentration in the precursor solution.

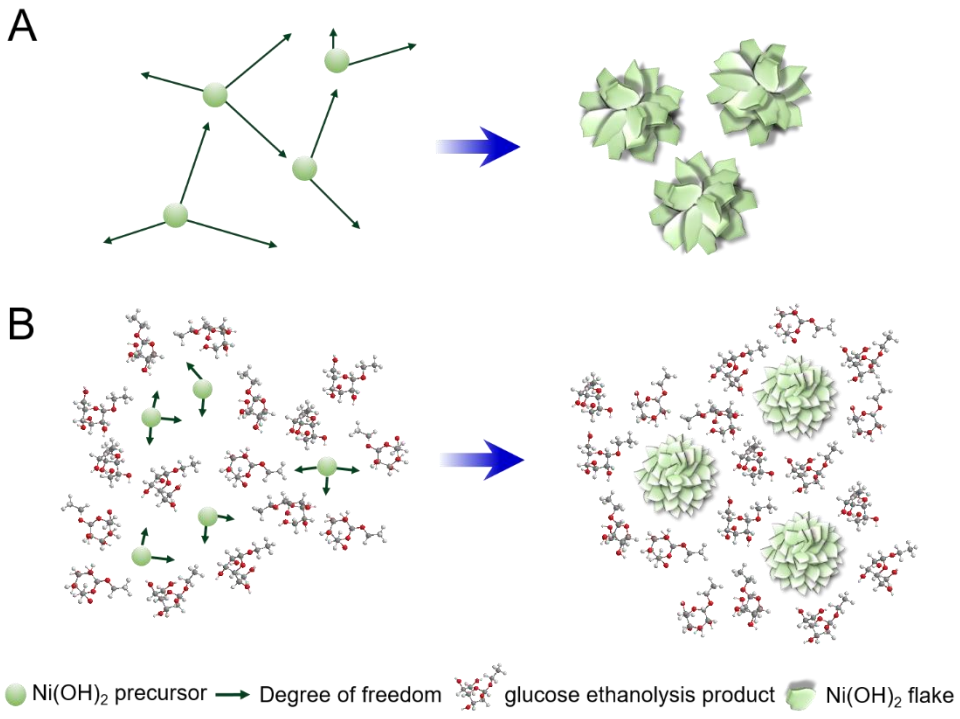

Figure 3: Schematic illustration of the proposed mechanism for the morphology modification of $Ni(OH)_2$ by glucose in the solvothermal medium. (A) $Ni(OH)_2$ precursors have sufficient spaces to diffuse and grow into large single crystals during synthesis without glucose. To reduce the surface energy, $Ni(OH)_2$ flakes aggregate forming a large-sized flower-like structure. (B) The ethanolysis products of glucose are suspended in the precursor solution. $Ni(OH)_2$ precursors have limited spaces for diffusion by ethyl glucosides. As a result, the size of the $Ni(OH)_2$ flower-like structure is significantly reduced.

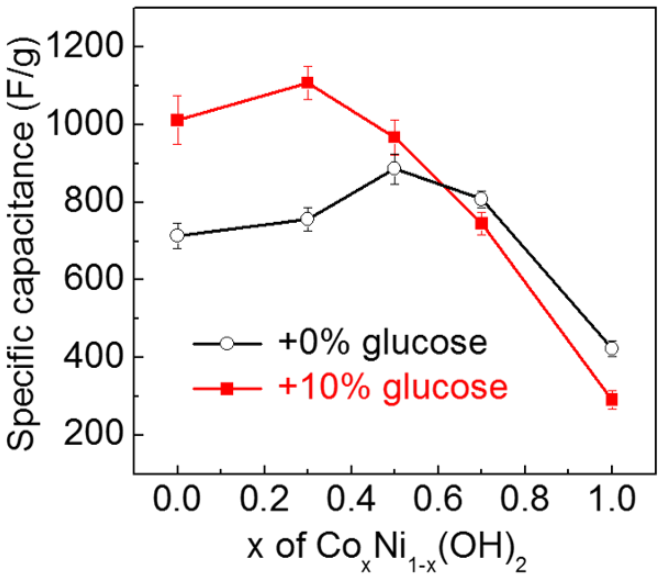

Figure 4: Trends in changes of the specific capacitance of $Co_xNi_{1-x}(OH)_2$ as functions of x. Each data point represents the average value of specific capacitance measured at a current density of 1 A g^{-1} and error bars represent the standard deviation.

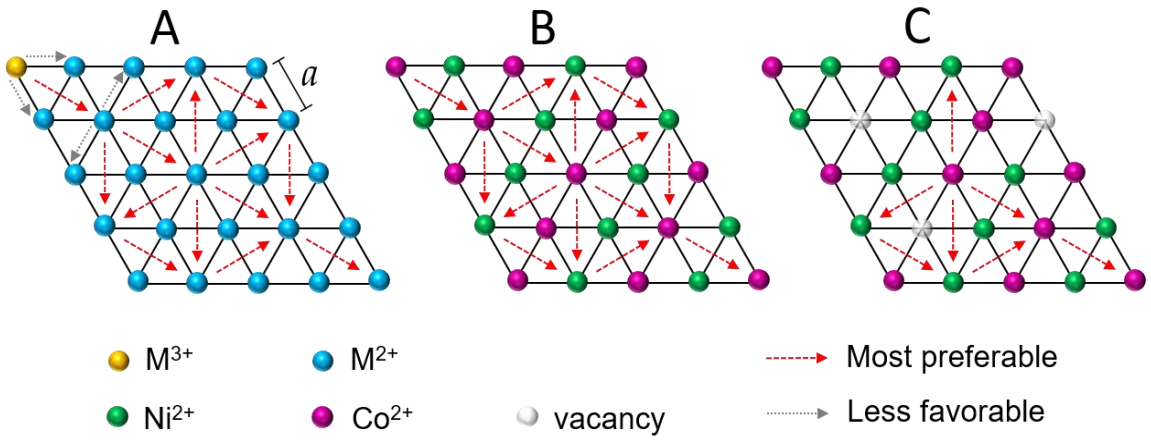

Figure 5: (A) Plausible edge-inward charge propagation directions from outermost edge site in a brucite sheet. Red arrows represent most preferable next-nearest neighboring hopping whereas gray arrows indicate less favorable nearest neighboring ones. (B) Charge propagation along the fastest next-nearest neighboring hopping in $Co_{0.5}Ni_{0.5}(OH)_2$ when charging. (C) Charge propagation in defective $Co_{0.5}Ni_{0.5}(OH)_2$ when charging. The distance between metal ions is represented as a. Modified based on ref 27.

The effect of morphology control over a wide range of Co doped-$Ni(OH)_2$ ($Co_xNi_{1-x}(OH)_2$, x = 0–1) was investigated. Interestingly, the specific capacitance improvement introduced by glucose was found to depend upon Co doping levels (**Figure 4**). It was more effective at low Co contents as compared to high Co contents. This tendency revealed the existence of competitive effects between chemical doping and morphology control. The possible reason for the competitive effect is the degree of inter-particle continuity and charge hopping. Specifically, more metal cation vacancies can exist on the surface of the highly amorphous materials, increasing the discontinuity between particles (**Figure 5**). Hence, in highly defective materials, the improvement due to charge hopping caused by chemical doping could become less effective. These findings will be important for effective electrode materials design for energy storage applications.

Influence of Nickel Oxide Nanostructure Morphology on the Effectiveness of Reduced Graphene Oxide Coating in Supercapacitor Electrodes[2]

Nickel oxide (NiO) has attractive qualities such as natural abundance, low cost, and high theoretical specific capacitance of 2583 F g^{-1}.[28] Because of its intrinsically poor electrical conductivity (~10^{-2}–10^{-4} S cm^{-1}), however, NiO-based electrodes have only reached a small part of their theoretical capacitance (200 − 600 F g^{-1}).[29-31] To solve this conductivity problem, considerable research efforts have been devoted to explore hybrid structures, where metal oxides are directly deposited on highly conductive metal nanostructures to improve the ion and electron transport in the electrode films.[32,33] Another approach is the use of conductive fillers mixed together with NiO in electrodes. Graphene and CNTs are among the most studied conductive fillers.[34-35]

[2] This work has been published in *J. Phys. Chem. C* **2014**, 118, 2281 – 2286.

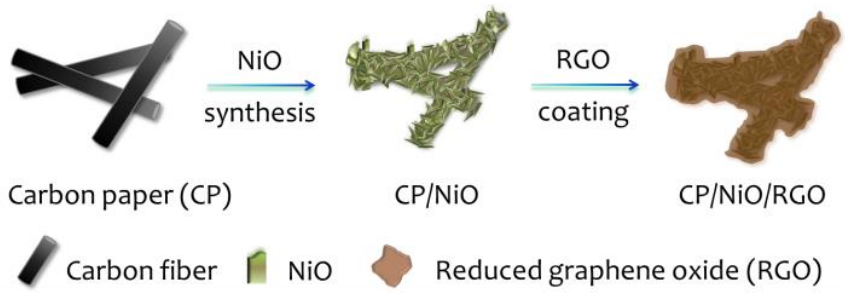

Figure 6: Schematic Illustration for Preparation of Reduced Graphene Oxide Coated NiO Grown on a Carbon Paper (CP).

We report a strategy for NiO-based supercapacitor electrodes with improved energy storage characteristics by introducing different types of carbons to NiO electrodes. First, to study the effects of reduced graphene oxide (RGO) coating, nanostructured NiO was grown on carbon paper (CP) and subsequently coated with RGO (**Figure 6**). We believe that the ultrathin layer of RGO sheets would provide an electron transport pathway in addition to the carbon paper substrate. EIS results showed enhanced conductivity after RGO coating (**Figure 7B**). Moreover, the addition of glucose during the solvothermal synthesis of NiO led to further increase in specific capacitance (**Figure 7A**). This increased specific capacitance can be explained by the following. Compared to the samples synthesized without glucose, both the size of NiO flakes and the thickness of NiO layer grown on the carbon paper were significantly reduced as results of adding glucose during synthesis. The reduced size and thickness are favorable for ion and electron transfer. Importantly, the mass loading of NiO was similar to that of NiO electrode synthesized without glucose. EIS measurement was indicative of improved conductivity due to the reduced length in ion and electron transfer paths (**Figure 7C**). RGO coating on this modified NiO electrode, however, showed only slight improvement in the specific capacitance since NiO is already utilized more effectively in this thinner film (**Figure 7A**). These results revealed that RGO coating is more effective in enhancing the specific capacitance of the electrode with poor

conductivity. Although RGO coating is less effective to improve specific capacitance of electrodes with high conductivity, it still enhanced the cycling stability by, presumably, improving its mechanical stability (**Figure 8**). This high cycling capacity implied that RGO coating provides the improved mechanical stability. SEM images of RGO-coated electrodes showed well-maintained structural integrity of the electrodes after long cycling.

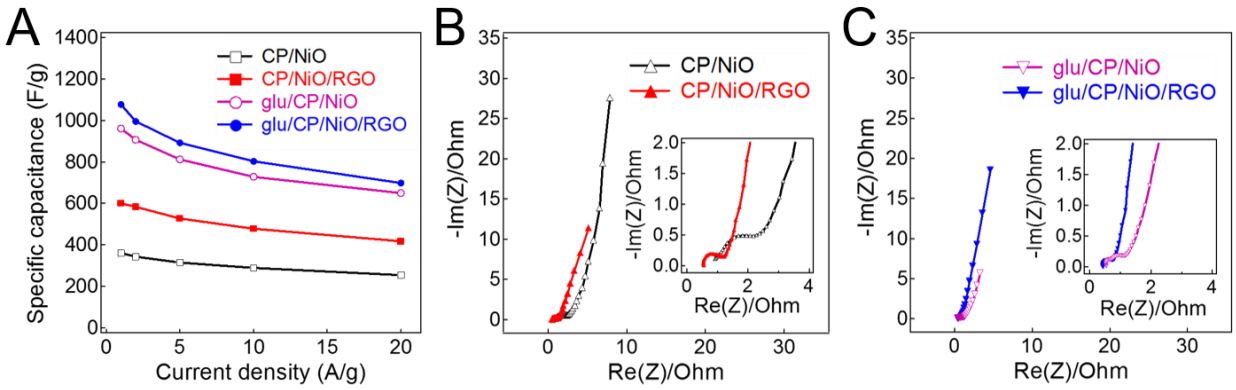

Figure 7: (A) Comparison of rate capabilities of CP/NiO/PVDF electrode, CP/NiO electrode, CP/NiO/RGO electrode, glu/CP/NiO electrode, and glu/CP/NiO/RGO electrode at different current densities of 1, 2, 5, 10, and 20 A g^{-1}, and Nyquist plots of (B) CP/NiO electrode and CP/NiO/RGO electrode and (C) glu/CP/NiO electrode and glu/CP/NiO/RGO electrode.

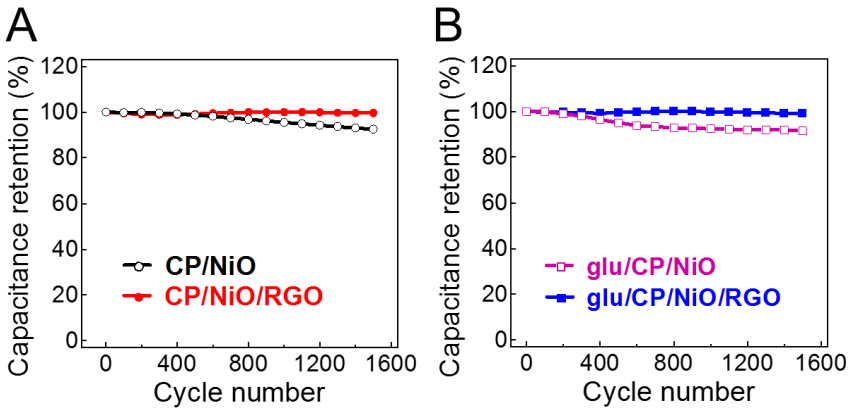

Figure 8: Comparison of cycling stability of (A) CP/NiO electrode and CP/NiO/RGO electrode and (B) glu/CP/NiO electrode and glu/CP/NiO/RGO electrode using CV conducted at a scan rate of 50 mV s^{-1}.

Effect of Interlayer Spacing on Sodium-Ion Insertion in Nanostructured Titanium Hydrogeno Phosphates/Carbon Nanotube Composites[3]

Titanium hydrogeno phosphates, of a formula $Ti(HPO_4)_2 \cdot xH_2O$, are built on a two-dimensional structure consisting of $PO_3(OH)$ tetrahedra and TiO_6 octahedra.[36] They have been proposed as possible Li- and Na-ion conductors through both cation exchange reactions and direct cation insertion into the structure.[37] The interlayer spacing of TiP-xH_2O varies with the amounts of water in the structure.[38] Recently, several groups reported the beneficial roles of water intercalation in layered structured electrode materials. The common conclusions from the earlier work is that water intercalation not only expands the interlayer spacing but also screens the strong interaction between elements in host layers and the charge carriers especially those with larger size or higher charge such as Na^+ and Mg^{2+}.[39,40] Therefore, water intercalation could improve the kinetics of charge mobility in the electrode as well as charge storage capacity and long term stability.[39,40] In this regard, the amenable interlayer properties with water intercalation provide sound rationale to explore applicability of TiP-xH_2O as electrode materials for Na-ion storage. Their Na-ion conduction and storage behaviors, however, have not been demonstrated. To the best of our knowledge, this is the first study on Na-ion storage in materials based on transition metal hydrogeno phosphates.

[3] This work has been submitted to *RSC adv*.

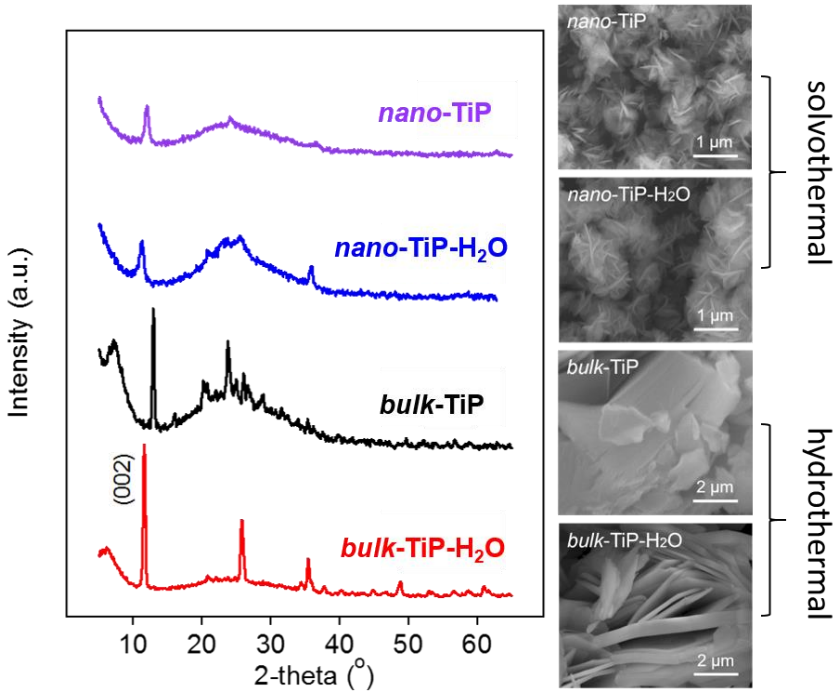

Figure 9: XRD patterns and SEM images of *bulk*-TiP-H_2O, *bulk*-TiP, *nano*-TiP-H_2O, and *nano*-TiP.

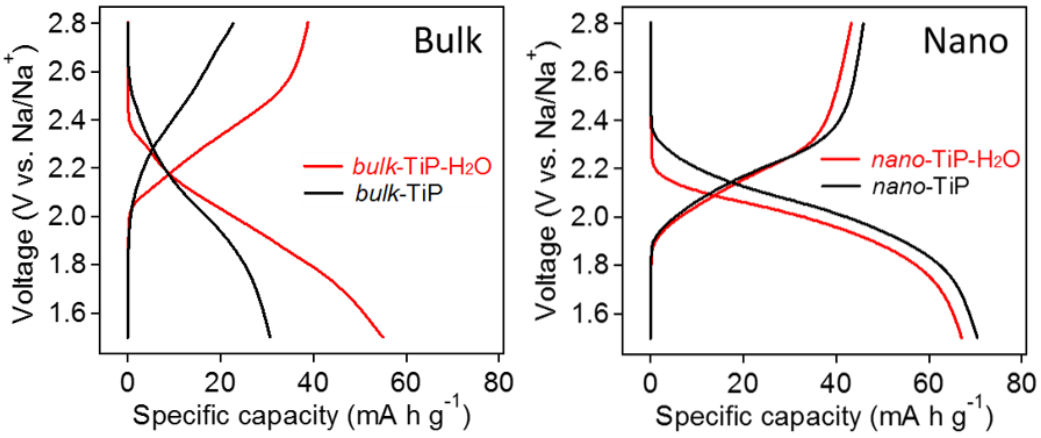

Figure 10: Comparisons of galvanostatic charge-discharge curves of *bulk*-TiP-H_2O, *bulk*-TiP, *nano*-TiP-H_2O, and *nano*-TiP.

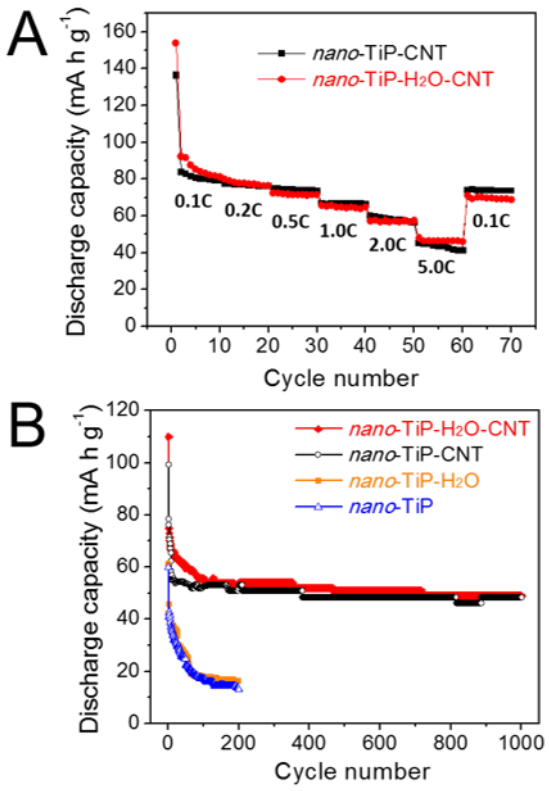

Figure 11: Comparisons of specific capacity of *nano*-TiP-H_2O-CNT and *nano*-TiP-CNT at various current rates of 0.1, 0.2, 0.5, 1.0, 2.0, and 5.0 C, (C) long cycle stability test results of *nano*-TiP-H_2O, *nano*-TiP, *nano*-TiP-H_2O-CNT, and *nano*-TiP-CNT at 2.0 C.

We investigated the reversible insertion of Na ions in bulk and nanostructured $Ti(HPO_4)_2{\cdot}xH_2O$ (*bulk*- and *nano*-TiP-xH_2O). The interlayer spacing of *bulk*- and *nano*-TiP-xH_2O was tuned with the amounts of water intercalation and the degree of crystallinity of samples was controlled by the synthesis routes (**Figure 9**). The expanded interlayer spacing with water intercalation incorporation enables better Na-ion diffusion in the *bulk*-TiP-H_2O materials (**Figure 10**). However, this beneficial effect of larger interlayer spacing was less pronounced when the size of TiP-xH_2O particles was reduced into nanoscale. Both hydrated and dehydrated *nano*-TiP-xH_2O displayed high specific capacity regardless the interlayer spacing (**Figure 10**). These results imply that ion diffusion in such nanostructured materials is likely independent of interlayer spacing varied with water intercalation. The electrochemical properties of *nano*-TiP-xH_2O

materials were further enhanced when prepared as composites with carbon nanotubes, exhibiting excellent rate capability, and long cycle stability (**Figure 11**).

NASICON Structured Materials for Sodium-Ion Batteries

The NASICON (Na-super-ionic conductors) structure has been receiving attention as solid electrolytes in Na/S-type batteries since the discovery in 1976.[41] The NASICON structure of general formula $A_xM_2(XO_4)_3$ is built on a 3-D framework of MO_6 octahedra linked with XO_4 tetrahedra.[42] The repeating unit of $M_2(XO_4)_3$ consists of three tetrahedra connected to two octahedra and is called 'lantern'. Based on these lantern units' arrangements, the NASICON structure can be described with either rhombohedral or monoclinic space groups.[42] Each lantern is connected to six other lanterns, forming large interstitials that can accommodate alkali cations.[42] This structural characteristic enables the fast ion transport in the NASICON framework as battery electrodes.

NASICON-type $NTi_2(PO_4)_3$ (NTP) has been considered as attractive NIB electrode due to its high theoretical capacity of 133 mA h g^{-1} (between 1.2 – 3.0 V), high Na-ion conductivity. NTP consists of $[TiO_6]$ octahedra sharing all the corners with $[PO_4]$ tetrahedra.[43] As NTP adopts NASICON structure, the 3-D open framework with plenty of interstitials capable of fast, reversible insertion and extraction of Na ions, showing high Na-ion conductivity. In addition, NASICON-type NTP is almost free from the volume change during Na insertion and extraction due to the structural stability provided by strong open framework. However, when considered as a NIB anode material, NTP shows relatively high redox potential at 2.1 V (vs. Na/Na^+) due to the inductive effect of phosphate groups. Despite the energy density loss associated with this

relatively higher redox potential, it not only enables safe quick charge but also reduces the possibility of forming a solid electrolyte interphase (SEI).[43]

However, NTP electrodes have low electrical conductivity, which limits electron transport kinetics within the electrode material and thus results in low capacity and poor rate capability.[44,45] To increase the transport kinetics of NTP electrodes, three main approaches have been used; reducing particle size to shorten the electron transport distance, doping other electroactive elements to improve transport properties, and mixing with carbons to improve electrode conductivity. Despite significant improvements with these approaches, achieving high capacity at high charge-discharge current rates is still challenging due to uncontrollable irregular morphology of NTP particles prepared by solid-state reactions.[46,47] Even though solid-state reactions are useful to synthesize NTP materials, these methods suffer from poly-dispersed crystal growth due to high processing temperatures, for example, at 900 ^{o}C.[48]

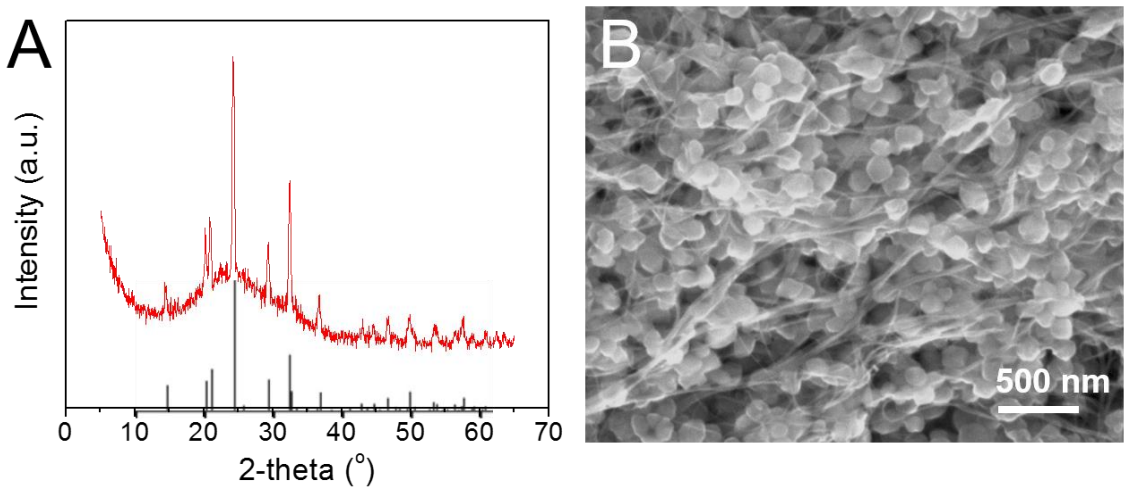

Figure 12: (A) XRD pattern and (B) SEM image of NTP/CNT composite synthesized via ethanol-mediated solvothermal reaction.

Figure 12A shows the XRD patterns of a NTP/CNT composite sample synthesized from the ethanol-mediated solvothermal reaction. All the peaks observed in the NTP/CNT composite

sample were well assigned to those of $NaTi_2(PO_4)_3$ (JCPDS No. 01-085-2265). The morphology and microstructure of the NTP/CNT composite were investigated using SEM. As shown in **Figure 12B**, uniform cube-like morphology was observed with a size of about 100 nm. These uniform morphology and size are favorable to form a well-mixed and connected composite with CNTs. Importantly, the size of the NTP particles in this work is much smaller than that of NTP particles synthesized via a solid-state reaction, where powder- or salt-type precursor chemicals are mechanically mixed followed by an annealing process at high temperatures between 800 and 900 ^{o}C.[49] For comparison, the NTP/CNT composite prepared from high temperature solid-state reaction shows irregular NTP particle shape and random size distribution. Such an irregular particle formation during the high temperature processing resulted in non-uniform mixing with CNTs.

The electrochemical performance of NTP/CNT composite electrode was evaluated using coin-type cells with a sodium metal foil as a counter electrode in 1 M $NaClO_4$ in EC/PC electrolyte. **Figure 13A** displays representative galvanostatic charge/discharge profiles of NTP/CNT at various current rates of 0.1, 0.2, 0.5, 1, 2, 5, 10, and 20 C within a cutoff voltage between 1.2 and 2.8 V. Well-defined charge-discharge voltage plateaus at ~2.10 V and ~2.15 V were clearly observed. These plateaus correspond to the redox reaction of the NTP/CNT composite electrode on the Ti^{3+}/Ti^{4+} couple that can be expressed as: $NaTi_2(PO_4)_3 + 2Na^+ + 2e^- \leftrightarrow Na_3Ti_2(PO_4)_3$.[44] NTP/CNT composite electrode showed excellent sodium storage capacity. The reversible capacities were 109, 97, 92, 88, 83, 77, 66, and 56 mA h g^{-1} at current rates of 0.1, 0.2, 0.5, 1, 2, 5, 10, and 20 C, respectively (**Figure 13B**). In addition, ~90% of discharge capacity is retained with a negligible polarization over the 90 cycles as shown in **Figure 13C**. Importantly, a reversible capacity of 56 mA h g^{-1} achieved even at a high current rate of 20 C is remarkable. At

this current rate, surprisingly, it took only 2 minutes and 13 seconds for a charge-discharge cycle of this NTP/CNT composite electrode.

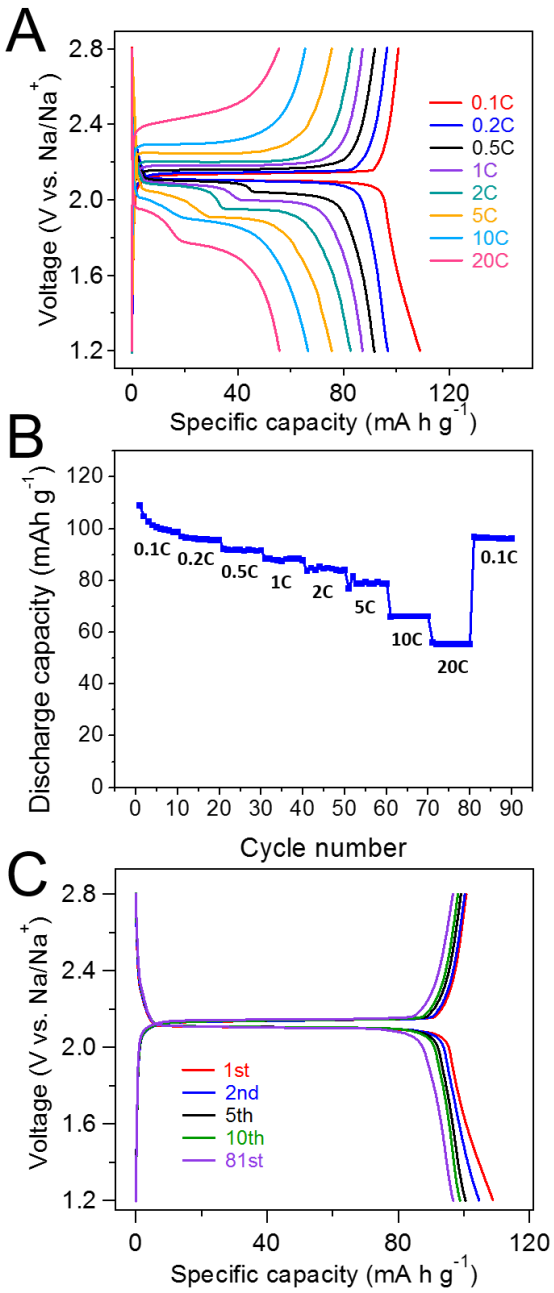

Figure 13: (A) Galvanostatic charge-discharge curves, (B) specific capacity of a NTP/CNT composite electrode at various current rates of 0.1, 0.2, 0.5, 1, 2, 5, 10, and 20 C, and (C) changes in the charge-discharge profile of a NTP/CNT composite electrode at a current rate of 0.1 C over cycles.

This fast rate performance is comparable to those of pseudocapacitance. In addition, 56 mA h g^{-1} is comparable to some reported capacity values achieved in 1 M Na_2SO_4 aqueous electrolyte with NTP/carbon composite electrodes at the same current rate. For example, the reversible capacity of a solvothermal processed NTP/graphene composite in 1 M Na_2SO_4 aqueous electrolyte was 40 mA h g^{-1} at 20 C.[44] Another NTP/graphene composite synthesized via solid-state reaction showed 63 mA h g^{-1} at 20 C in 1 M Na_2SO_4 aqueous electrolyte.[50] Considering the lower ionic conductivity and higher viscosity of the organic solvent-based electrolyte compared to those of aqueous counterparts, our preliminary results are promising, indicating that the NTP/CNT composite electrode can achieve high energy and power density simultaneously. According to Yang *et al.*, regular morphology can allow preferable surface for ion diffusion to be exposed in all individual particles.[46] In the case of irregular morphology, however, the preferable surface is not always available for the fastest ion diffusion. Thus, the uniformly controlled morphology and size of NTP particles could also contribute to the improvement in electrochemical performances.

NASICON structures provide rigid and strong 3-D channels for fast ion conduction. Such stable structures, compared to simple metal oxides, could be used as multivalent ion storage applications. However, multivalent ions such as Mg^{2+} show slow diffusion kinetics due to the strong interaction with atoms in electrode materials. Since NASICON structures consist of metal cations with higher oxidation states that can interact stronger with anions in the electrode material, these materials can improve ion diffusion kinetics. NASICON-type $Mg_{0.5}Ti_2(PO_4)_3$ (MTP) was prepared and evaluated as LIB electrode materials first. NASICON-type MTP was synthesized via a high temperature sintering process. Typically, stoichiometric amounts of magnesium acetate, titanium butoxide, and ammonium dihydrogen phosphate were mixed in DI

water at 75 ^{o}C to get a powder product. Then, the powder product was sintered at 900 ^{o}C in Ar atmosphere for 12 h. Electrochemical Li-ion half-cell tests were performed using CR 2032-type coin cells. A piece of lithium metal foil were used as a counter electrode, and 1 M $LiPF_6$ in EC and diethyl carbonate (DEC) (1/1 = v/v) was used as an electrolyte. **Figure 14A** shows an XRD pattern of as-synthesized MTP material. The observed peaks were identified as the pattern of MTP in R-3c space group.[51] **Figure 14B** shows electrochemical Li-ion insertion into as-prepared MTP electrode film at 0.1 C. The plateaus observed between 2.8 and 2.0 V are reversible during further discharge. These plateaus can be originated from Ti^{4+}/Ti^{3+} redox couple, while lithium ions are reversibly inserted in the structure. This electrochemical Li-ion insertion shows potentials for the use of MTP as electrode materials for other battery systems.

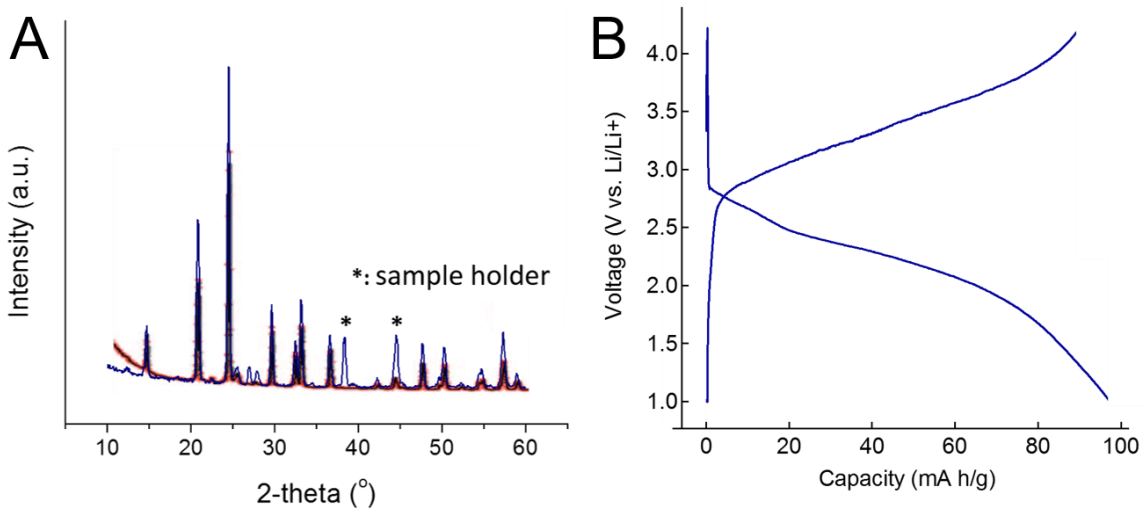

Figure 14: (A) XRD pattern of as-synthesized MTP. Peaks from XRD sample holder were marked as *, and (B) charge and discharge capacity of as-prepared MTP electrodes at 0.1 C.

References

1. A. C. Dillon, *Chem. Rev.*, 2010, **110**, 6856-6872.
2. J. W. Long, D. Bélanger, T. Brousse, W. Sugimoto, M. B. Sassin and O. Crosnier, *MRS Bull.*, 2011, **36**, 513-522.
3. OECD Environmental Outlook to 2050, Chapter 3.
4. H. Chen, T. N. Cong, W. Yang, C. Tan, Y. Li and Y. Ding, *Prog. Nat. Sci.*, 2009, **19**, 291-312.
5. M. Winter and R. J. Brodd, *Chem. Rev.*, 2004, **104**, 4245-4269.
6. D. S. Su and R. Schlogl, *ChemSusChem*, 2010, **3**, 136-168.
7. L. L. Zhang and X. S. Zhao, *Chem. Soc. Rev.*, 2009, **38**, 2520-2531.
8. P. Simon and Y. Gogotsi, *Nat. Mater.*, 2008, **7**, 845-854.
9. C. Hu, K. Chang, M. Lin and Y. Wu, *Nano Lett.*, 2006, **6**, 2690-2695.
10. X. C. Dong, H. Xu, X. W. Wang, Y. X. Huang, M. B. Chan-Park, H. Zhang, L. H. Wang, W. Huang and P. Chen, *ACS Nano*, 2012, **6**, 3206-3213.
11. Y. Cheng, S. Lu, H. Zhang, C. V. Varanasi and J. Liu, *Nano Lett.*, 2012, **12**, 4206-4211.
12. M. Sathiya, A. S. Prakash, K. Ramesha, J. M. Tarascon and A. K. Shukla, *J. Am. Chem. Soc.*, 2011, **133**, 16291-16299.
13. G. F. Cai, J. P. Tu, J. Zhang, Y. J. Mai, Y. Lu, C. D. Gu and X. L. Wang, *Nanoscale*, 2012, **4**, 5724-5730.
14. V. Etacheri, R. Marom, R. Elazari, G. Salitra and D. Aurbach, *Energy Environ. Sci.*, 2011, **4**, 3243.
15. H. Kang, Y. Liu, K. Cao, Y. Zhao, L. Jiao, Y. Wang and H. Yuan, *J. Mater. Chem. A*, 2015, **3**, 17899-17913.
16. N. Yabuuchi, K. Kubota, M. Dahbi and S. Komaba, *Chem. Rev.*, 2014, **114**, 11636-11682.
17. H. Xiong, M. D. Slater, M. Balasubramanian, C. S. Johnson and T. Rajh, *J. Phys. Chem. Lett.*, 2011, **2**, 2560-2565.
18. J. W. Lee, T. Ahn, D. Soundararajan, J. M. Ko and J. D. Kim, *Chem. Commun.*, 2011, **47**, 6305-6307.
19. P. Olivia, J. Leonardi and J. F. Laurent, *J. Power Sources*, 1982, ***8***, 229-255.
20. G. Wang, L. Zhang and J. Zhang, *Chem. Soc. Rev.*, 2012, **41**, 797-828.
21. Y. Cheng, H. Zhang, C. V. Varanasi and J. Liu, *Energy Environ. Sci.*, 2013, **6**, 3314-3321.
22. J. Huang, T. Lei, X. Wei, X. Liu, T. Liu, D. Cao, J. Yin and G. Wang, *J. Power Sources*, 2013, **232**, 370-375.
23. Z. You, K. Shen, Z. Wu, X. Wang and X. Kong, *Appl. Surf. Sci.*, 2012, **258**, 8117-8123.
24. X. Liu, R. Ma, Y. Bando and T. Sasaki, *Adv. Mater.*, 2012, **24**, 2148-2153.
25. L. Xie, Z. Hu, C. Lv, G. Sun, J. Wang, Y. Li, H. He, J. Wang and K. Li, *Electrochim. Acta*, 2012, **78**, 205-211.
26. C. Liu, F. Li, L. P. Ma and H. M. Cheng, *Adv. Mater.*, 2010, **22**, E28-62.
27. R. Ma, J. Liang, X. Liu and T. Sasaki, *J. Am. Chem. Soc.*, 2012, **134**, 19915-19921.
28. W. Deng, X. Ji, Q. Chen and C. E. Banks, *RSC Adv.*, 2011, **1**, 1171.

29. C. Y. Cao, W. Guo, Z. M. Cui, W. G. Song and W. Cai, *J. Mater. Chem.*, 2011, **21**, 3204.
30. X.-h. Xia, J.-p. Tu, X.-l. Wang, C.-d. Gu and X.-b. Zhao, *J. Mater. Chem.*, 2011, **21**, 671-679.
31. Z. Zhu, J. Ping, X. Huang, J. Hu, Q. Chen, X. Ji and C. E. Banks, *J. Mater. Sci.*, 2011, **47**, 503-507.
32. G. W. Yang, C. L. Xu and H. L. Li, *Chem. Commun.*, 2008, **48**, 6537-6539.
33. H. Wang, Q. Pan, X. Wang, G. Yin and J. Zhao, *J. Appl. Electrochem.*, 2009, **39**, 1597-1602.
34. W. Lv, F. Sun, D.-M. Tang, H.-T. Fang, C. Liu, Q.-H. Yang and H.-M. Cheng, *J. Mater. Chem.*, 2011, **21**, 9014.
35. M.-S. Wu, Y.-P. Lin, C.-H. Lin and J.-T. Lee, *J. Mater. Chem.*, 2012, **22**, 2442-2448.
36. S. Bruque, M. A. G. Aranda, E. R. Losilla, P. Olivera-Pastor and P. Maireles-Torres, *Inorg. Chem.*, 1995, **34**, 893-899.
37. V. Pralong, V. Caignaert and B. Raveau, *J. Mater. Chem.*, 2011, **21**, 12188-12201.
38. R. Llavona, M. SuBrez, J. R. Garza and J. Rodriguez, *Inorg. Chem.*, 1989, **28**, 2863-2868.
39. K. W. Nam, S. Kim, S. Lee, M. Salama, I. Shterenberg, Y. Gofer, J. S. Kim, E. Yang, C. S. Park, J. S. Kim, S. S. Lee, W. S. Chang, S. G. Doo, Y. N. Jo, Y. Jung, D. Aurbach and J. W. Choi, *Nano Lett.*, 2015, **15**, 4071-4079.
40. K. W. Nam, S. Kim, E. Yang, Y. Jung, E. Levi, D. Aurbach and J. W. Choi, *Chem. Mater.*, 2015, **27**, 3721-3725.
41. H. Y. P. Hong, *Mater. Res. Bull.*, 1976, **11**, 173-182.
42. C. Masquelier and L. Croguennec, *Chem. Rev.*, 2013, **113**, 6552-6591.
43. G. Pang, P. Nie, C. Yuan, L. Shen, X. Zhang, H. Li and C. Zhang, *J. Mater. Chem. A*, 2014, **2**, 20659-20666.
44. G. Pang, C. Yuan, P. Nie, B. Ding, J. Zhu and X. Zhang, *Nanoscale*, 2014, **6**, 6328-6334.
45. Y. Jiang, J. Shi, M. Wang, L. Zeng, L. Gu and Y. Yu, *ACS Appl. Mater. Interfaces*, 2016, **8**, 689-695.
46. J. Yang, H. Wang, P. Hu, J. Qi, L. Guo and L. Wang, *Small*, 2015, **11**, 3744-3749.
47. C. Wu, P. Kopold, Y. L. Ding, P. A. van Aken, J. Maier and Y. Yu, *ACS Nano*, 2015, **9**, 6610-6618.
48. K. Saravanan, P. Balaya, M. V. Reddy, B. V. R. Chowdari and J. J. Vittal, *Energy Environ. Sci.*, 2010, **3**, 457.
49. W. Wu, J. Yan, A. Wise, A. Rutt and J. F. Whitacre, *J. Electrochem. Soc.*, 2014, **161**, A561-A567.
50. X. Li, X. Zhu, J. Liang, Z. Hou, Y. Wang, N. Lin, Y. Zhu and Y. Qian, *J. Electrochem. Soc.*, 2014, **161**, A1181-A1187.
51. C. Vidal-Abarca, J. M. Ateba Mba, C. Masquelier, J. L. Tirado, and P. Lavela, *J. Electrochem. Soc.*, 2012, **159**, A1716-A1721.